



SHEAR BEHAVIOR OF STRUCTURAL LIGHTWEIGHT CONCRETE BEAMS

Ashraf Ragab¹, Khalid Helal², Sherif Elwan³, and Ayman Khalil⁴

¹ Research Assistant, Structural Engineering Department, Higher Institute of Engineering, Cairo, EGYPT

² Associate Professor, Structural Engineering Department, Ain Shams University, Cairo, EGYPT

³ Assistant Professor, Civil Engineering Department, Higher Institute of Engineering, Cairo, EGYPT

⁴ Professor, Structural Engineering Department, Ain Shams University, Cairo, EGYPT

ملخص البحث

يقدم البحث دراسة سلوك القص للكمرات ذات الخرسانة خفيفة الوزن المعرضة لحمل مركز في نقطتين. تم عمل نموذج عنصر محدود باستخدام حزمة الكمبيوتر (ANSYS Ver.10) والتحقق منه واستخدامه بشكل واسع في دراسة تأثير عوامل مختلفة.

ABSTRACT

This research program was conducted to investigate the shear behaviour of structural lightweight concrete beams subjected to two-point load. For this purpose, a finite element model using the computer package ANSYS Ver.10 was developed, verified, and implemented in an extensive parametric study.

All the necessary steps to create the models which are prepared to investigate the behaviour of structural lightweight concrete beams in shear. The experimental results for shear of structural LWC beams presented by Wessam Antar et al. [1]. The experimental results were compared with finite element results to verify the accuracy of finite element models.

A verification of the finite element model was conducted to ensure that the proposed elements, material properties, real constants, and convergence criteria are adequate to model the response of the beam.

A total of twenty-four beams (all beams are simply supported) were analysed. The analysed beams were chosen to investigate the effect of various parameters including using structural lightweight concrete instead of ordinary concrete, variation of shear reinforcement, and variation of cross section of the beams.

1. INTRODUCTION

Lightweight concrete is of utmost importance to the construction industry. Most of current concrete research focuses on high-performance concrete, by which is meant a cost-effective material that satisfies demanding performance requirements, including durability. The advantages of lightweight concrete are its reduced mass and improved thermal and sound insulation properties, while maintaining adequate strength. The reduced weight has numerous advantages, not the least of them being a reduced demand on energy during construction.

Data collection from several research work has been done at Ain Shams University including testing of lightweight concrete beams in flexure, shear, etc. However, little numerical models were developed to expand the experimental findings to

a parametric study. In order to benefit from the available test data done at Ain Shams University and elsewhere a calibrated finite element model will be developed to model the behaviour of lightweight concrete beams subjected to shear stress.

This paper investigates the effect of various parameters including using structural lightweight concrete instead of ordinary concrete, variation of shear reinforcement, and variation of the shape of the beams on the shear behaviour of beams. In this respect, a total of twenty-four simply supported beams were analysed.

2. FINITE ELEMENT ANALYSIS

2.1. VERIFICATION OF ANSYS PROGRAM

Finite element modeling using the software package ANSYS10. All the necessary steps to create the models which are prepared to investigate the behavior of structural lightweight concrete beams in shear. The experimental results for shear of structural LWC beams presented by Wessam Antar et al.

The experimental results were compared with finite element results to verify the accuracy of finite element models.

All beams had a rectangular cross section of 150 mm wide and 300 mm total depth. The beam effective depth was set to 275 mm. The clear span of the tested beams was fixed for all beams to be 2000 mm but the total length of beams was 2300 mm.

All beams were tested under two-point load. All specimens detail are listed in Table (1) and shown in Figures (1.a) and (1.b).

Table 1. Specimens details

Specimen	Total Span (mm)	Clear Span (mm)	Longitudinal Steel at Total Length	Add Long. Steel at Each Support	Stirrups	Concrete Strength (N/mm ²)
B1	2300	2000	4 Ø 16	-----	5 Ø 6/m'	25
B2	2300	2000	4 Ø 16	2 Ø 16	5 Ø 6/m'	25
B3	2300	2000	4 Ø 16	2 Ø 18	5 Ø 6/m'	25
B4	2300	2000	4 Ø 16	1 Ø 18 ----- 1 Ø 18	5 Ø 6/m'	25
B5	2300	2000	4 Ø 16	1 Ø 16 1 Ø 12 1 Ø 16	5 Ø 6/m'	25
B6	2300	2000	4 Ø 16	1 Ø 16 1 Ø 12 1 Ø 16	-----	25
B7	2300	2000	4 Ø 16	2 Ø 16	5 Ø 6/m'	40
B8	2300	2000	4 Ø 16	2 Ø 18	5 Ø 6/m'	40

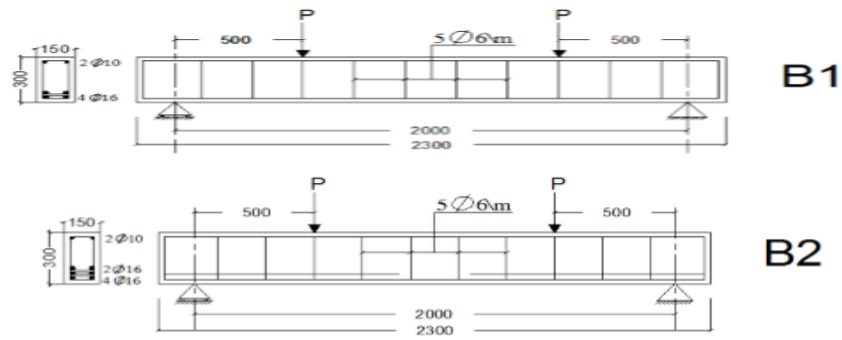


Figure 1.a Reinforcement and concrete dimensions of beams (B1 and B2) tested under shear (dimension in mm).

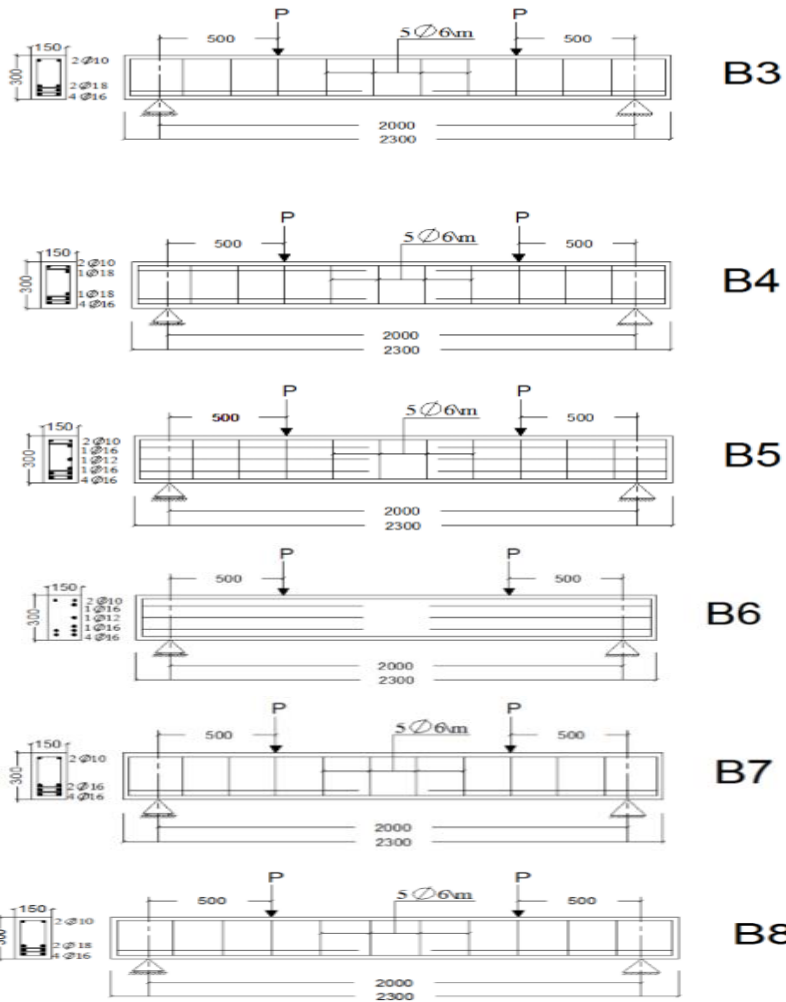


Figure 1.b Reinforcement and concrete dimensions of beams (B3, B4, B5, B6, B7 and B8) tested under shear (dimension in mm).

2.1.1. FAILURE LOADS

The experimental and finite element failure loads are compared in Table (2)

Table 2. Failure loads

Specimen	EXP. Failure Load (KN)	F.E. Failure Load (KN)	VFE/VEXP
B1	100	108	1.08
B2	110	112	1.02
B3	125	116	0.93
B4	120	114.5	0.95
B5	95	117.6	1.24
B6	50	71.3	1.43
B7	110	161.5	1.47
B8	130	163.8	1.26

2.1.2. LOAD-DEFLECTION

As shown in Figures (2), (3), (4), (5), (6), (7), (8), and (9), the numerical models gave load versus mid span deflection in good agreement with the experimental one.

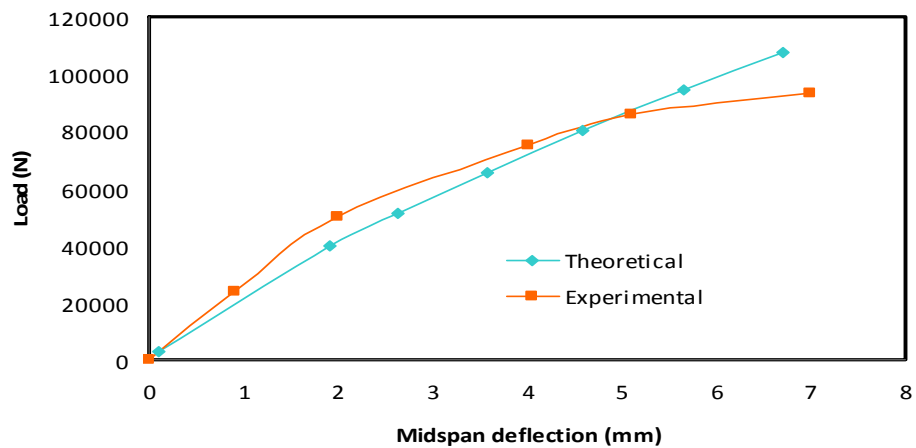


Figure 2. Experimental and numerical load versus mid span deflection plots of B1.

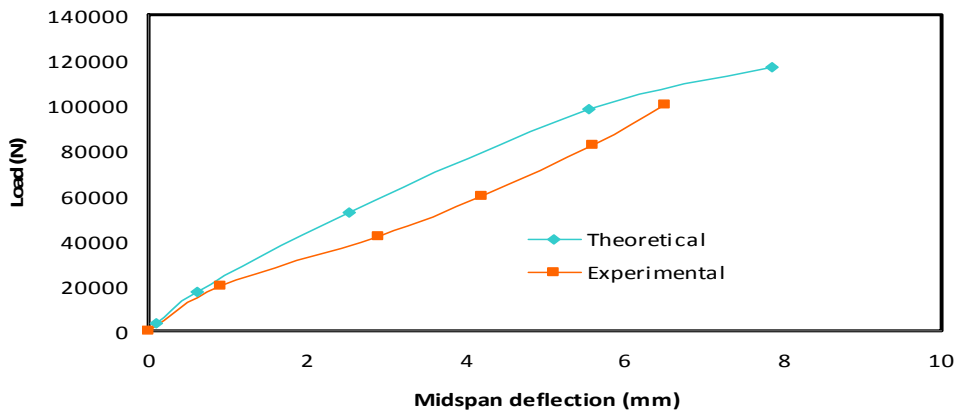


Figure 3. Experimental and numerical load versus mid span deflection plots of B2.

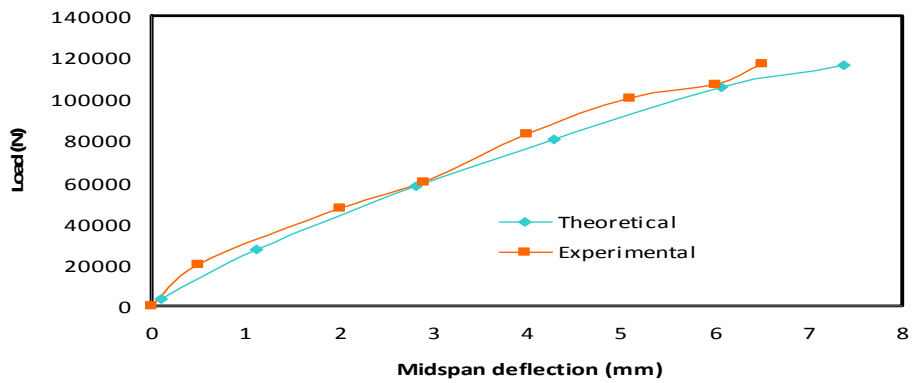


Figure 4. Experimental and numerical load versus mid span deflection plots of B3.

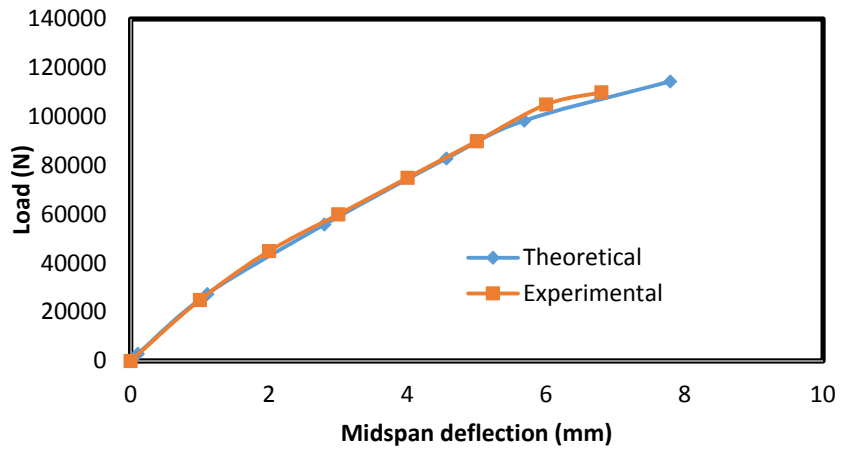


Figure 5. Experimental and numerical load versus mid span deflection plots of B4.

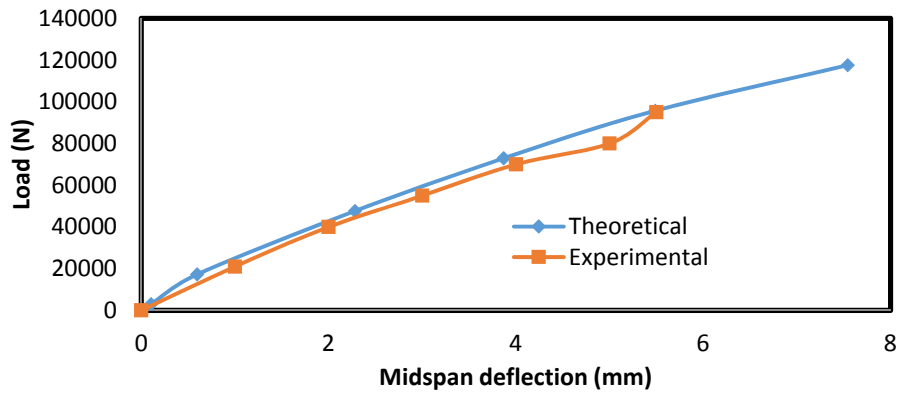


Figure 6. Experimental and numerical load versus mid span deflection plots of B5.

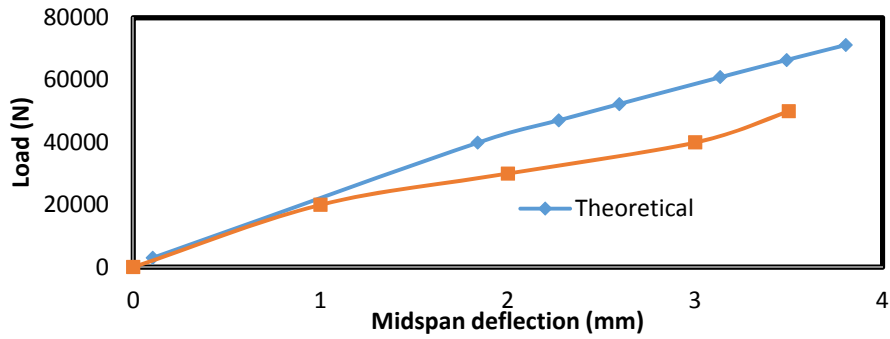


Figure 7. Experimental and numerical load versus mid span deflection plots of B6.

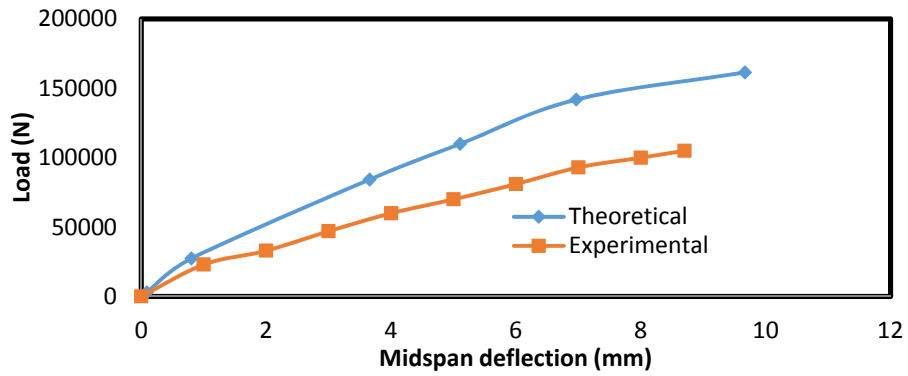


Figure 8. Experimental and numerical load versus mid span deflection plots of B7.

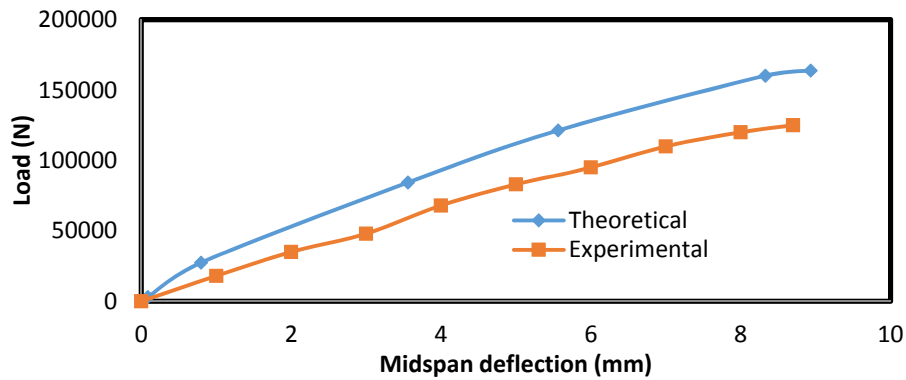


Figure 9. Experimental and numerical load versus mid span deflection plots of B8.

2.2. PARAMETRIC STUDY

2.2.1. DESCRIPTION OF THE ANALYZED BEAMS

Loading and Boundary Conditions, All the tested beams were simply supported and loaded by two-point load.

Geometry, Figure (10) is shown the cross-section for all the tested beams.

Reinforcement, Table (3) is shown the reinforcement for all the tested beams.

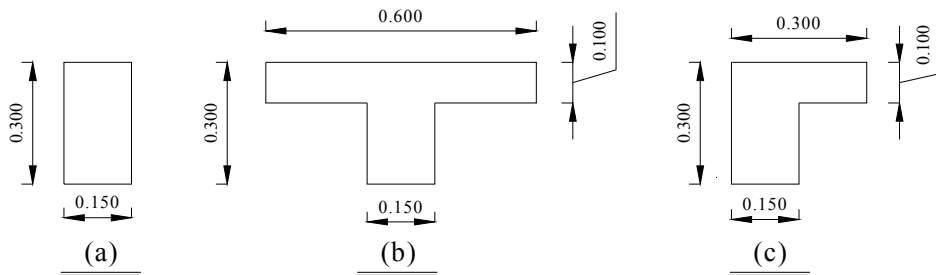


Figure 10. Cross-section for all the tested beams (a) group 1, (b) group 2, and (c) group 3.

Table 3. Description of the analyzed beams

Group	Type of Sec.	Type of Conc.	Model	Total Span (mm)	Clear Span (mm)	Long. Steel at Total Leng. (Bott.)	Long. Steel at Mid. Span (Top)	Long. Steel at Each Sup. (Top)	Add Long. Steel at Each Sup.	Stirrups (/m')	
										At Sup.	At Span
1	Rec. Sec.	LWC	B1	2300	2000	4 Ø 16	2 Ø 10	2 Ø 10	-----	5 Ø 6	5 Ø 6
			B2	2300	2000	4 Ø 16	2 Ø 10	2 Ø 10	2 Ø 16	5 Ø 6	5 Ø 6
			B3	2300	2000	4 Ø 16	2 Ø 10	2 Ø 10	2 Ø 18	5 Ø 6	5 Ø 6
			B4	2300	2000	4 Ø 16	2 Ø 10	2 Ø 10	2 Ø 18	-----	-----
		O.C.	B5	2300	2000	4 Ø 16	2 Ø 10	2 Ø 10	-----	5 Ø 6	5 Ø 6
			B6	2300	2000	4 Ø 16	2 Ø 10	2 Ø 10	2 Ø 16	5 Ø 6	5 Ø 6
			B7	2300	2000	4 Ø 16	2 Ø 10	2 Ø 10	2 Ø 18	5 Ø 6	5 Ø 6
			B8	2300	2000	4 Ø 16	2 Ø 10	2 Ø 10	2 Ø 18	-----	-----
2	T - Sec.	LWC	B9	2300	2000	4 Ø 16	2 Ø 10	2 Ø 10	-----	5 Ø 6	5 Ø 6
			B10	2300	2000	4 Ø 16	2 Ø 10	2 Ø 10	2 Ø 16	5 Ø 6	5 Ø 6
			B11	2300	2000	4 Ø 16	2 Ø 10	2 Ø 10	2 Ø 18	5 Ø 6	5 Ø 6
			B12	2300	2000	4 Ø 16	2 Ø 10	2 Ø 10	2 Ø 18	-----	-----
		O.C.	B13	2300	2000	4 Ø 16	2 Ø 10	2 Ø 10	-----	5 Ø 6	5 Ø 6
			B14	2300	2000	4 Ø 16	2 Ø 10	2 Ø 10	2 Ø 16	5 Ø 6	5 Ø 6
			B15	2300	2000	4 Ø 16	2 Ø 10	2 Ø 10	2 Ø 18	5 Ø 6	5 Ø 6
			B16	2300	2000	4 Ø 16	2 Ø 10	2 Ø 10	2 Ø 18	-----	-----
3	L - Sec.	LWC	B17	2300	2000	4 Ø 16	2 Ø 10	2 Ø 10	-----	5 Ø 6	5 Ø 6
			B18	2300	2000	4 Ø 16	2 Ø 10	2 Ø 10	2 Ø 16	5 Ø 6	5 Ø 6
			B19	2300	2000	4 Ø 16	2 Ø 10	2 Ø 10	2 Ø 18	5 Ø 6	5 Ø 6
			B20	2300	2000	4 Ø 16	2 Ø 10	2 Ø 10	2 Ø 18	-----	-----
		O.C.	B21	2300	2000	4 Ø 16	2 Ø 10	2 Ø 10	-----	5 Ø 6	5 Ø 6
			B22	2300	2000	4 Ø 16	2 Ø 10	2 Ø 10	2 Ø 16	5 Ø 6	5 Ø 6
			B23	2300	2000	4 Ø 16	2 Ø 10	2 Ø 10	2 Ø 18	5 Ø 6	5 Ø 6
			B24	2300	2000	4 Ø 16	2 Ø 10	2 Ø 10	2 Ø 18	-----	-----

2.2.2. MATERIAL PROPERTIES

The concrete for the tested beams was assumed to have a characteristic strength of $f_{cu} = 25$ MPa while its ultimate rupture tensile strength (f_{ctr}) was taken equal to $0.6\sqrt{f_{cu}}$ MPa as recommended by ECP-203. Also, the longitudinal reinforcement and the stirrups were assumed to behave as an elastic perfectly plastic material with yield stresses equal to 360 MPa and 240 MPa, respectively.

2.2.3. DETERMINATION OF REINFORCEMENT

The reinforcement in each beam was determined in a way that satisfies the required tension and compression reinforcement ratios. The procedure, which was suggested to determine the areas of steel, was:

Step (1): Calculation of the maximum area of steel

The maximum area of steel (A_{smax}) was taken equal to ($\mu_{max} \times b \times d$), where, μ_{max} is the maximum reinforcement ratio for ($\gamma_c=1.0$ and $\gamma_s=1.0$) and is taken equal to ($1.5 \times 5 \times 10^{-4} f_{cu}$) for yield stress of steel equal to 360 MPa, and b , and d are the breadth and effective depth of the beam, respectively.

Step (2): Calculation of area of tension and compression reinforcement

- Assume a value for compression to tension reinforcement ratio (α) = 0.2.
- Assume a value for tension to maximum reinforcement ratio (R) = 0.33.
- Calculate the value of A_s , and A_s' from:
 $(A_s - A_s') / A_{smax} = R$ and $A_s' = \alpha A_s$.

Step (3): Calculation of the maximum load capacity

- Compute the height of compression zone, c from: $0.67 f_{cu} b a + A_s' f_s' = A_s f_s$.
- Where, $a = 0.8c$, f_s and f_s' are the stresses in tension and compression reinforcement, respectively and for case of under reinforced sections, they may be replaced by the yield stress, f_y .
- Check strain in compressive reinforcement and determine the corresponding stress f_{sc} ($f_{sc} = f_y$ for $\epsilon_s' \geq \epsilon_y$ and $f_{sc} = E_s \epsilon_s'$ otherwise).
- Compute moment capacity, M_u from: $M_u = A_s f_y (d - a/2) + A_s' f_{sc} (a/2 - d')$, d' (concrete cover) = 50 mm.
- Compute load capacity, P_u from: $P_u = M_u \times 4/L$.

Step (4): Calculate area of stirrups

- Determine the applied shear force, Q_u from: $Q_u = W_u (L/2 - c/2 - d/2)$, c (breadth of support) = 300 mm.
- Determine the applied shear stress, q_u from: $q_u = Q_u / (bd)$.
- Determine the shear stress carried by concrete, q_{cu} from: $q_{cu} = 0.24 \sqrt{f_{cu}}$
- Determine the shear stress carried by stirrups, q_{st} from:
 $q_{st} = q_u - 0.5 q_{cu}$.
- Compute the required area of one branch of stirrups, A_{str} from:
 $A_{str} = q_{st} \times b \times s / f_{yst}$, s (spacing between stirrups) = 200 mm.

The values of A_s , A_s' and A_{str} for each group were calculated as mentioned above and presented in Table (3).

3. RESULTS

3.1. CRACK PATTERNS AND MODES OF FAILURE

3.1.1 CRACK INITIATION AND PROPAGATION

The first crack that appeared in all beams was of flexural type, and this was followed by vertical cracks at maximum moment region. These vertical cracks

propagated towards the two ends of the beam as the applied load was increased. New diagonal cracks were then developed beside the supports. These cracks continued until the ultimate load. At this stage, the cracks continued to grow excessively wide leading to final failure. At failure, some crushing of the concrete appeared at the top of the maximum moment region of the beam. According to the previous description of the cracks in all beams, the failure mode of such beams may be classified as shear type.

3.1.2 CRACK PATTERN

The cracking patterns of the beams obtained from ANSYS were plotted as shown in Figures (11 and 12).

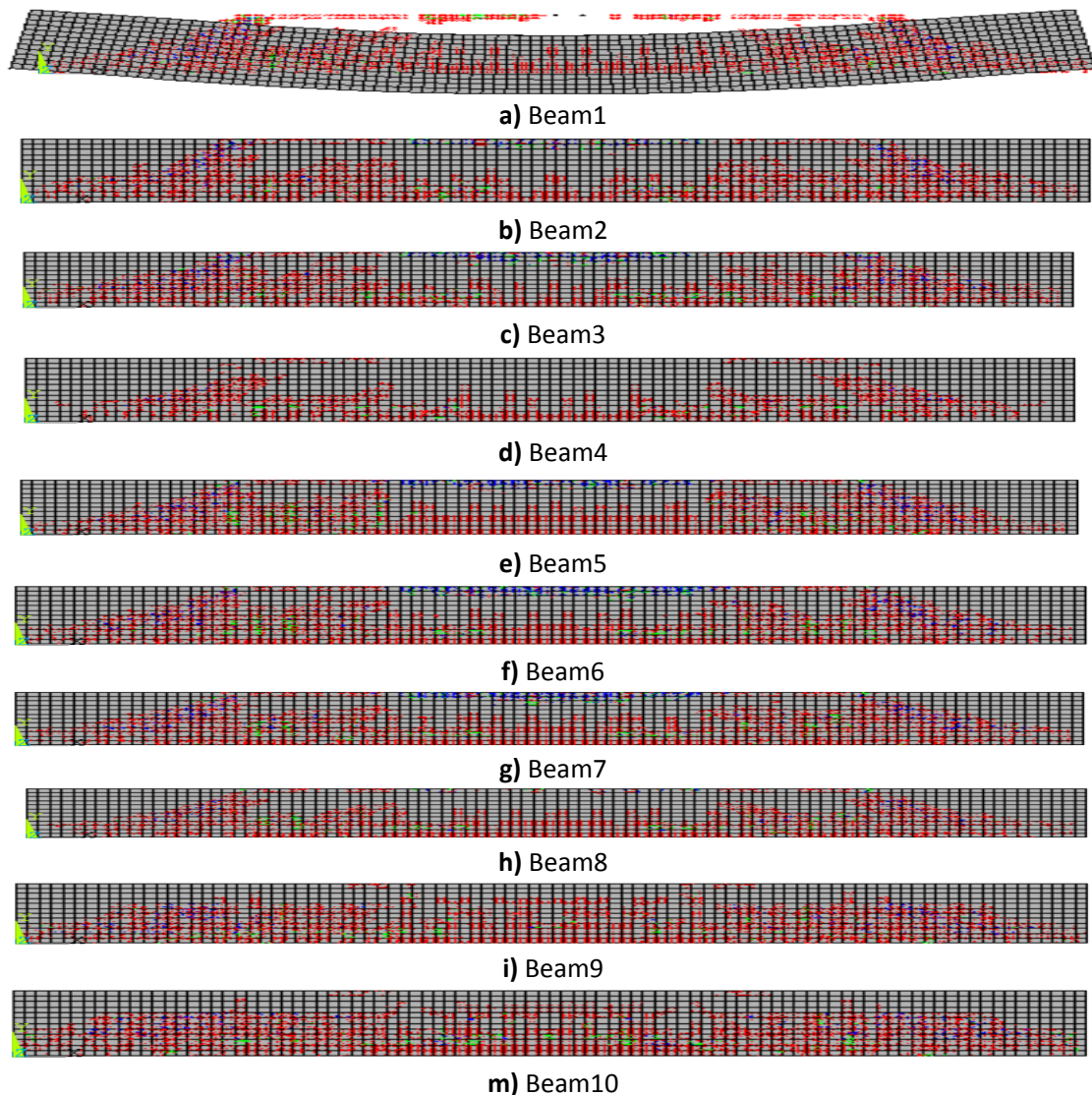
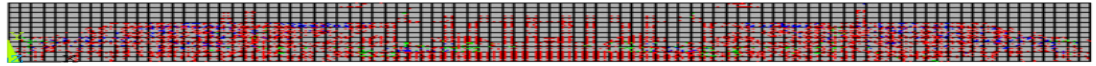


Figure 11. Crack patterns of beams 1, 2, 3, 4, 5, 6, 7, 8, 9, and 10.



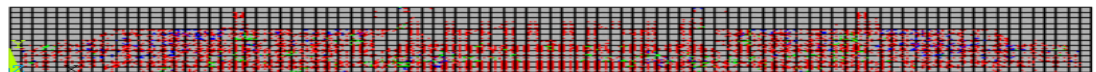
a) Beam11



b) Beam12



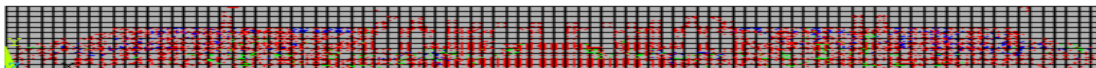
c) Beam13



d) Beam14



e) Beam15



f) Beam16



g) Beam17



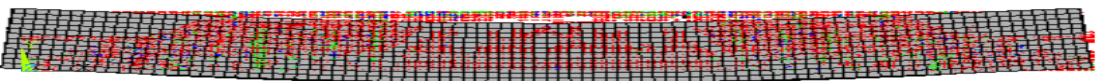
h) Beam18



i) Beam19



m) Beam20



n) Beam21



k) Beam22



l) Beam23



v) Beam24

Figure 12. Crack patterns of beams 11, 12, 13, 14, 15, 16, 17, 18, 19, 20, 21, 22, 23, and 24.

3.2. LOADS AT FAILURE

The failure load of all modeled beams is presented in Table (4). It may be seen that in general, Providing shear reinforcement in reinforced concrete beam increases its ultimate capacity in shear. The increasing in the failure load depends also on the type of concrete and cross section. Some of these parameters have major effect and others have minor effect.

Table 4. The failure load of all modeled beams

Specimen	F.E. Failure Load (KN)	Specimen	F.E. Failure Load (KN)
B1	108	B13	142.6
B2	112	B14	143.5
B3	116	B15	146.1
B4	88.4	B16	140.4
B5	99	B17	131.2
B6	101.6	B18	133.3
B7	104.1	B19	135
B8	85	B20	125.2
B9	146	B21	121
B10	149.9	B22	123.8
B11	153.4	B23	126.6
B12	145.4	B24	116.2

3.3. LOAD-DEFLECTION CURVES

Figures (13 to 24) show the effect of the investigated parameters on the load deflection curves of all modeled beams. It can be seen that these curves have common characteristics, where each curve consists of four zones: zone A represents the behavior before cracking, zone B represents the behavior during cracking, zone C represents the behavior after cracking, and zone D represents the behavior approaching failure load. The stiffness of beams, as represented by the slope of the load deflection curve, is significantly affected by using structural lightweight concrete instead of ordinary concrete.

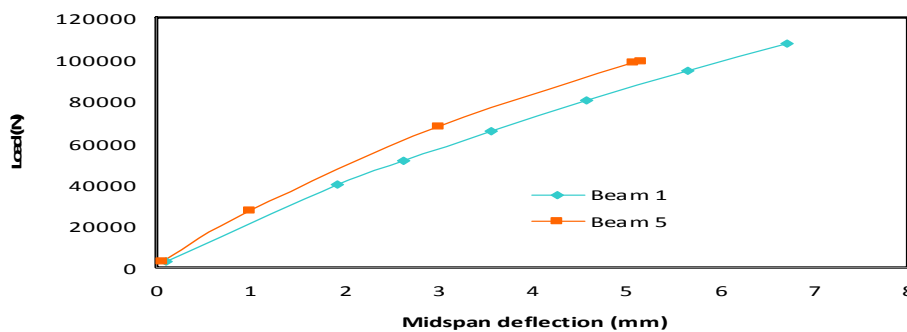


Figure 13. Load-deflection curve of beams (1) and (5).

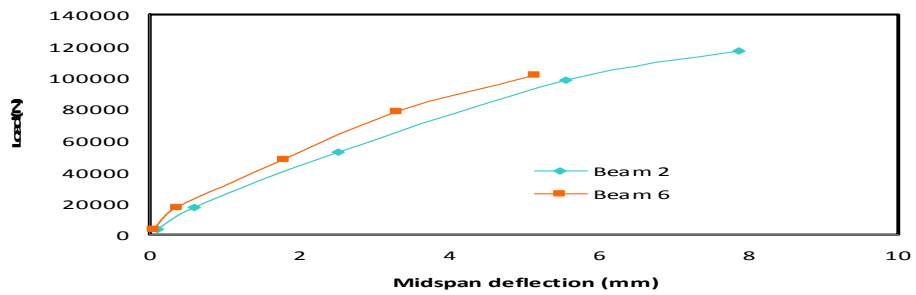


Figure 14. Load-deflection curve of beams (2) and (6).

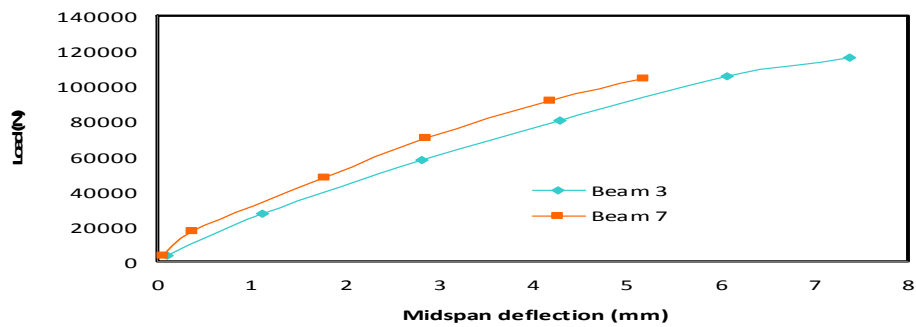


Figure 15. Load-deflection curve of beams (3) and (7).

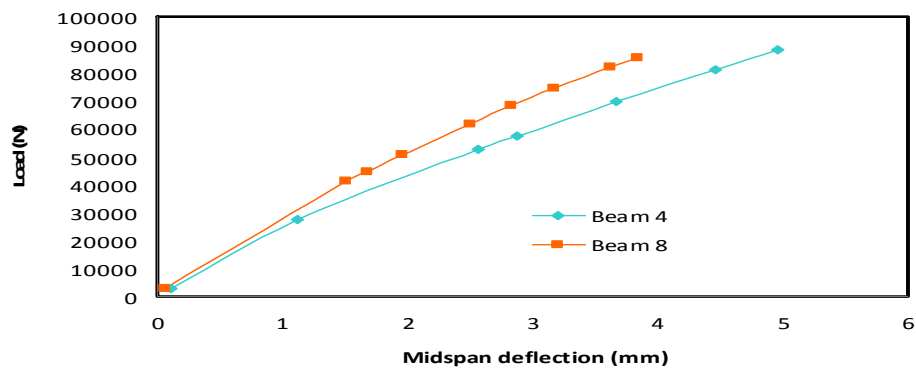


Figure 16. Load-deflection curve of beams (4) and (8).

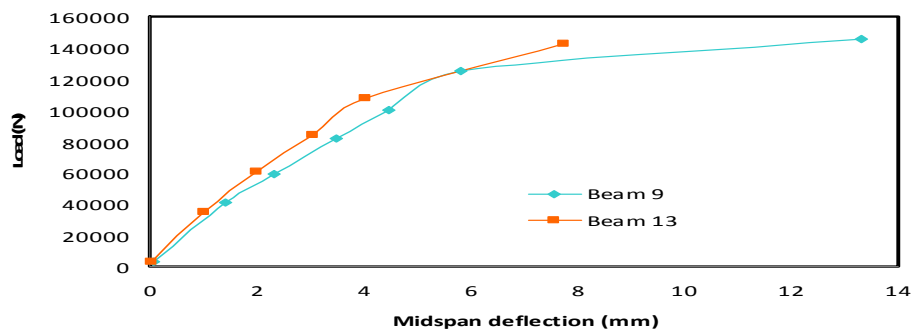


Figure 17. Load-deflection curve of beams (9) and (13).

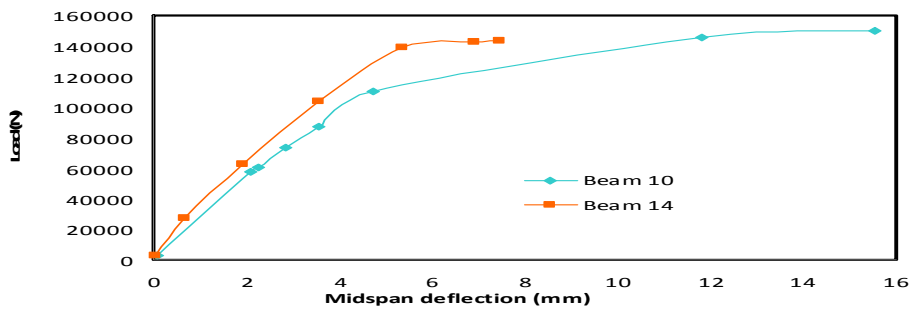


Figure 18. Load-deflection curve of beams (10) and (14).

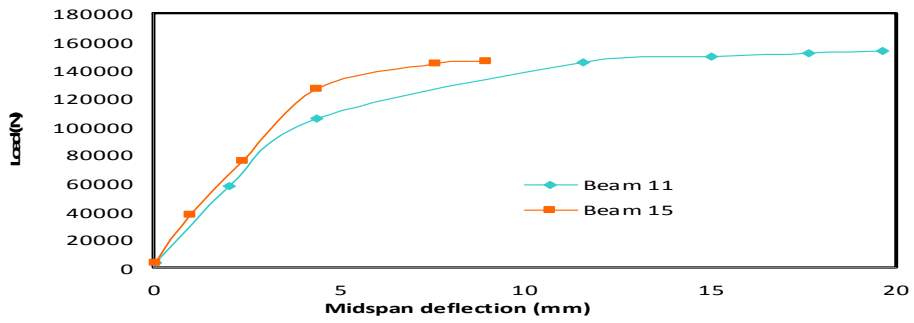


Figure 19. Load-deflection curve of beams (11) and (15).

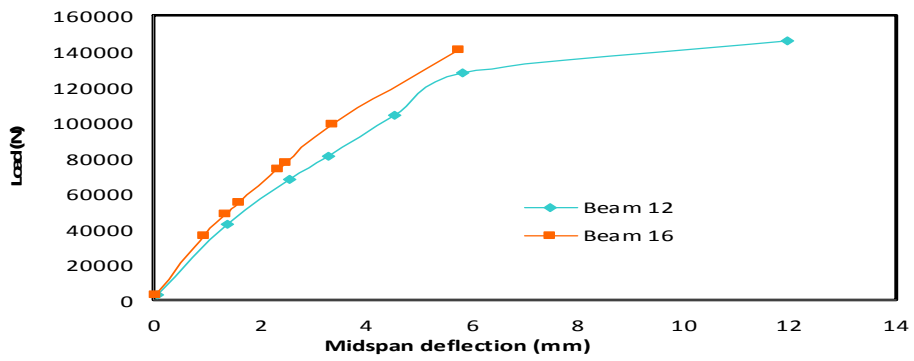


Figure 20. Load-deflection curve of beams (12) and (16).

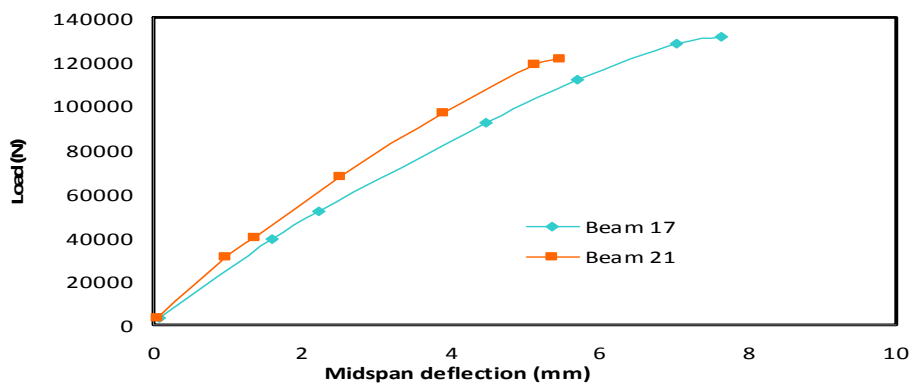


Figure 21. Load-deflection curve of beams (17) and (21).

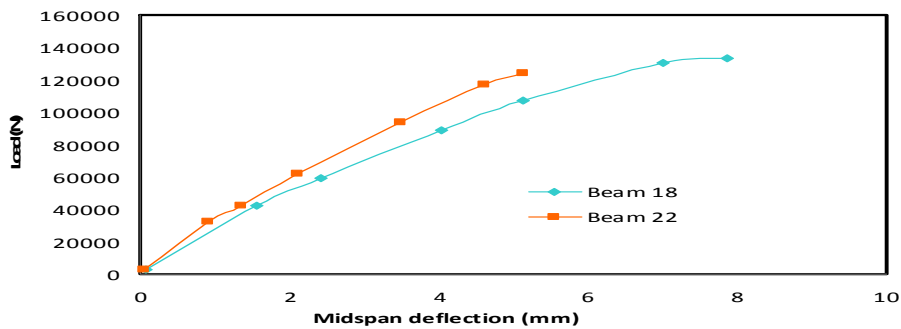


Figure 22. Load-deflection curve of beams (18) and (22).

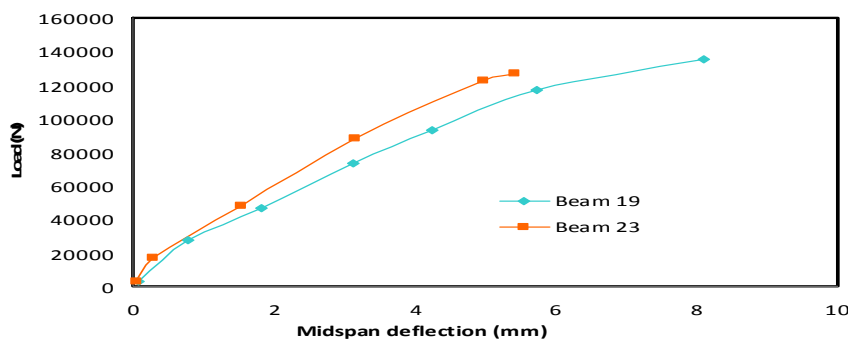


Figure 23. Load-deflection curve of beams (19) and (23).

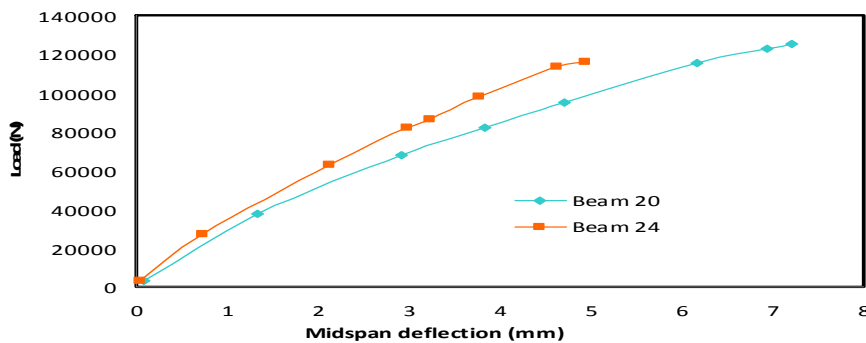


Figure 24. Load-deflection curve of beams (20) and (24).

4. CONCLUSIONS

This paper investigated the shear behavior of structural lightweight concrete beams. Based on the analysis of results obtained from finite element modeling of simply supported reinforced-concrete beams, several conclusions are drawn as given below:

4.1 Effect of using LWC instead of ordinary concrete

1. The failure mode of such beams may be classified as diagonal tensile failure mode.
2. Insignificant enhancement in the ultimate load occurred when using structural lightweight concrete instead of ordinary concrete by percentage not more than 10%.

4.2 Effect of variation of shear reinforcement

1. Providing main RFT dowel action (with $\mu = 63.5\%$ from main RFT) increases its ultimate capacity in shear by percentage not more than 7%.

2. Using main RFT dowel action (with $\mu = 63.5\%$ from main RFT) instead of stirrups reduces its ultimate capacity in shear by percentage not more than 30%.
3. Using main RFT dowel action (with $\mu = 63.5\%$ from main RFT) instead of stirrups has minor effect on the stiffness of beams.

4.3 Effect of the shape of the beam

1. Increasing in the ultimate load occurred when using L-section (with $B/b=2$) instead of R-section by not more than 30%.
2. Increasing in the ultimate load occurred when using T-section (with $B/b=4$) instead of R-section by not more than 40%.
3. At ultimate load reduction in the stiffness occurred when using lightweight concrete instead of ordinary concrete by percentage not more than 24% for R-Section and L-Section (with $B/b=2$) and 14% for T-Section (with $B/b=4$).
4. At ultimate load providing main RFT dowel action (with $\mu = 63.5\%$ from main RFT) increases the stiffness of beams by percentage not more than 43% for R-Section, 11% for L-Section (with $B/b=2$) and 17% for T-Section (with $B/b=4$).
5. Increasing in the stiffness of beams occurred when using L-section (with $B/b=2$) instead of R-section by not more than 15% and 20% when using T-section (with $B/b=4$).

5. REFERENCES

- Eiad Hafiz Zahran, "Studying the Behavior of Slender Reinforced Lightweight Concrete Columns Subjected to Eccentric Loads," International Journal of Engineering and Applied Sciences (IJEAS), Vol. 3, Issue 4, ISSN: 2394 -3661, April 2016.
- A. Farghal Maree, and K. Hilal Riad, "Analytical and Experimental Investigation for Bond Behavior of Newly Developed Polystyrene Foam Particles Lightweight Concrete," Elsevier Science Direct Journal, Vol. 58, pp. 1-11, January 2014.
- El-Sayed M. Anter, A. H. Zaher, Amgad A. Talat, and Omar A. El-Nawawy, "Flexural Behavior of Reinforced Lightweight Concrete Beams Provided with Tension Bar Splices," M.Sc. Thesis, Ain Shams University, Cairo, Egypt, 2014.
- Wessam, A. M., "Shear of Structural Lightweight Concrete Beams," M.Sc. Thesis, Ain Shams University, Cairo, Egypt, 2012.
- K. Salah, A. Talaat, and A. H. Khalil, "Effect of Openings on Shear Behavior of Lightweight Concrete Deep Beams," M.Sc. Thesis, Ain Shams University, Cairo, Egypt, 2012.
- ACI 318-14 (2002), "Building Code Requirements for Structural Concrete and Commentary," ACI Committee 318, American Concrete Institute, Farmington Hills, Michigan, USA, 2002, 443 pp.
- ACI 213R-03 (2003), "Guide for Structural Lightweight-Aggregate Concrete," ACI Committee 213 Report, American Concrete Institute, Farmington Hills, Michigan, USA, 2003, 38 pp.

- ECCS 203-01 (2007), “Egyptian Code of Practice for Design and Construction of Concrete Structures,” Second Edition, Egyptian National Housing and Building Research Center, Giza, Egypt, 2001, 334 pp.
- ANSYS (2005), ANSYS User’s Manual Revision 5.5, ANSYS, Inc., Canonsburg, Pennsylvania, US.
- Document BE96-3942/R2 (1998), “LWAC Material Properties-State-of-the-Art,” EuroLightCon Document BE96-3942/R1, Project Funded by the European Union under the Industrial & Materials Technologies Programme (Brite-EuRam III), Contract BRPR-CT97-0381, Project BE96-3942, December 1998.